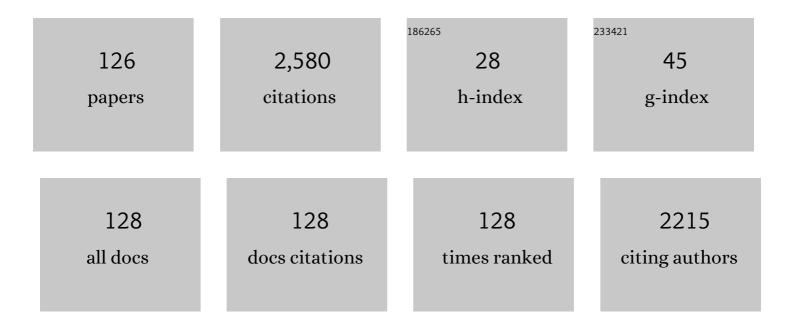
List of Publications by Year in descending order

Source: https://exaly.com/author-pdf/8152639/publications.pdf Version: 2024-02-01



#	Article	IF	CITATIONS
1	First-principles design and experimental validation of β-Ti alloys with high solid-solution strengthening and low elasticities. Materials Science & Engineering A: Structural Materials: Properties, Microstructure and Processing, 2022, 843, 143053.	5.6	9
2	Ceramic science of crystal defect cores. Journal of the Ceramic Society of Japan, 2022, 130, 648-667.	1.1	34
3	Formation of Extra Vacancies in Nucleating γ Phase during Îʿ-γ Massive-like Phase Transformation in Carbon Steel. Journal of Smart Processing, 2021, 10, 202-207.	0.1	0
4	Heat transport through propagon-phonon interaction in epitaxial amorphous-crystalline multilayers. Communications Physics, 2021, 4, .	5.3	8
5	Surface segregation of 3 mol % yttria-doped tetragonal zirconia particle studied by atomic-resolution scanning transmission electron microscopy-energy-dispersive X-ray spectroscopy. Journal of the Ceramic Society of Japan, 2021, 129, 561-565.	1.1	4
6	Direct numerical analyses of nanoscale thermal transport near MgO edge dislocations. Scripta Materialia, 2021, 202, 113991.	5.2	4
7	Substantial role of charge transfer on the diffusion mechanism of interstitial elements in α-titanium: A First-principles study. Scripta Materialia, 2021, 203, 114065.	5.2	12
8	Highâ€Density Frenkel Defects as Origin of Nâ€Type Thermoelectric Performance and Low Thermal Conductivity in Mg <sub>3</sub> Sb <sub>2</sub> â€Based Materials. Advanced Functional Materials, 2021, 31, 2008469.	14.9	38
9	Grain-size dependence and anisotropy of nanoscale thermal transport in MgO. Applied Physics Letters, 2021, 119, .	3.3	6
10	Role of phonons on phase stabilization of RE2Si2O7 over wide temperature range (RE = Yb, Gd). Journal of the European Ceramic Society, 2020, 40, 780-788.	5.7	8
11	Time-resolved and <i>In-situ</i> Observation of <i>Î́</i> – <i>γ</i> Transformation during Unidirectional Solidification in Fe–C Alloys. ISIJ International, 2020, 60, 930-938.	1.4	5
12	Quantitative prediction of grain boundary thermal conductivities from local atomic environments. Nature Communications, 2020, 11, 1854.	12.8	46
13	Recent Progress in Nanostructured Functional Materials and Their Applications. Materials Transactions, 2020, 61, 2435-2441.	1.2	3
14	Transformation from Ferrite to Austenite during/after Solidification in Peritectic Steel Systems: an X-ray Imaging Study. ISIJ International, 2020, 60, 2755-2764.	1.4	12
15	Dendrite fragmentation induced by massive-like Î′–γ transformation in Fe–C alloys. Nature Communications, 2019, 10, 3183.	12.8	65
16	Atomistic mechanisms of thermal transport across symmetric tilt grain boundaries in MgO. Acta Materialia, 2019, 171, 154-162.	7.9	24
17	Time-resolved and <i>In-situ</i> Observation of δ-γ Transformation during Unidirectional Solidification in Fe-C Alloys. Tetsu-To-Hagane/Journal of the Iron and Steel Institute of Japan, 2019, 105, 290-298.	0.4	14
18	Investigation using 4D-CT of massive-like transformation from the δ to γ phase during and after δ-solidification in carbon steels. IOP Conference Series: Materials Science and Engineering, 2019, 529, 012013.	0.6	11

#	Article	IF	CITATIONS
19	Selection of the Massive-like <i>δ</i> - <i>γ</i> Transformation due to Nucleation of Metastable <i>δ</i> Phase in Fe-18 Mass%Cr-Ni Alloys with Ni Contents of 8, 11, 14 and 20 Mass%. ISIJ International, 2019, 59, 459-465.	1.4	13
20	Firstâ€principles study in an interâ€granular glassy film model of silicon nitride. Journal of the American Ceramic Society, 2018, 101, 2673-2688.	3.8	23
21	Atomistic simulations of grain boundary transformation under high pressures in MgO. Physica B: Condensed Matter, 2018, 532, 2-8.	2.7	16
22	Native point defects in MoS 2 and their influences on optical properties by first principles calculations. Physica B: Condensed Matter, 2018, 532, 184-194.	2.7	11
23	Electrochemical Properties of Fe Solid-Solution Strengthened Sintered Titanium. Funtai Oyobi Fummatsu Yakin/Journal of the Japan Society of Powder and Powder Metallurgy, 2018, 65, 761-765.	0.2	0
24	Hierarchically Structured Thermoelectric Materials in Quaternary System Cu–Zn–Sn–S Featuring a Mosaic-type Nanostructure. ACS Applied Nano Materials, 2018, 1, 2579-2588.	5.0	13
25	Density functional study of the phase stability and Raman spectra of Yb <sub>2</sub> O <sub>3</sub> , Yb <sub>2</sub> SiO <sub>5</sub> and Yb <sub>2</sub> Si <sub>2</sub> O <sub>7</sub> under pressure. Physical Chemistry Chemical Physics, 2018, 20, 16518-16527.	2.8	30
26	X-Ray Imaging of Formation and Growth of Spheroidal Graphite in Ductile Cast Iron. Materials Science Forum, 2018, 925, 104-109.	0.3	5
27	Quantifying Anharmonic Vibrations in Thermoelectric Layered Cobaltites and Their Role in Suppressing Thermal Conductivity. Scientific Reports, 2018, 8, 11152.	3.3	18
28	<i>In Situ</i> Observations of Tensile and Compressive Deformations in Semi Solid Metallic Alloys Using Time-resolved X-ray Imaging. Tetsu-To-Hagane/Journal of the Iron and Steel Institute of Japan, 2017, 103, 668-677.	0.4	5
29	Elucidation of Mechanism of Emergence of Magnetic Anisotropy in FePd by Phase-Field Modeling. Journal of the Japan Society for Precision Engineering, 2017, 83, 415-419.	0.1	0
30	A density functional theory study of electronic and magnetic properties of rare earth doped monolayered molybdenum disulphide. Journal of Applied Physics, 2016, 120, .	2.5	32
31	Preface to Special Topic: Cutting Edge Physics in Functional Materials. Journal of Applied Physics, 2016, 120, 142001.	2.5	2
32	Controlling the electronic properties of Gd: MoS2 monolayer with perpendicular electric field. Journal of Electroceramics, 2016, 37, 29-33.	2.0	6
33	Isolated energy level in the band gap of <mml:math xmlns:mml="http://www.w3.org/1998/Math/MathML"&gt; <mml:mrow> <mml:msub> <mml:mi>Yb </mml:mi> <mml:m mathvariant="normal"&gt;O  <mml:mn>7 </mml:mn> </mml:m </mml:msub> </mml:mrow> identified by electron energy-loss spectroscopy. Physical Review B, 2016, 93, .</mml:math 	ny23.2	ıl:mn>
34	Atomically ordered solute segregation behaviour in an oxide grain boundary. Nature Communications, 2016, 7, 11079.	12.8	105
35	Direct Visualization of the Grain Boundary Solute Segregation in Oxide Material at Atomic Resolution Using STEM-EDS. Microscopy and Microanalysis, 2016, 22, 1340-1341.	0.4	Ο
36	Role of nitrogen vacancies in cerium doped aluminum nitride. Journal of Magnetism and Magnetic Materials, 2016, 412, 49-54.	2.3	15

#	Article	IF	CITATIONS
37	A density functional theory study of electronic properties of substitutional alloying of monolayer MoS 2 and CeS 2 surface models. Computational and Theoretical Chemistry, 2016, 1084, 98-102.	2.5	4
38	Manipulating Thermal Conductivity by Interfacial Modification of Misfit-Layered Cobaltites Ca3Co4O9. Journal of Electronic Materials, 2016, 45, 1217-1226.	2.2	12
39	Numerically-quantified two dimensionality of microstructure evolution accompanying variant selection of FePd. Materials Research Express, 2015, 2, 076502.	1.6	1
40	Impacts of Interface Energies and Transformation Strain from BCC to FCC on Massive-like δ-γ Transformation in Steel. IOP Conference Series: Materials Science and Engineering, 2015, 84, 012049.	0.6	10
41	Interface Energies of Hetero- and Homo-Phase Boundaries and Their Impact on δ-γ Massive-Like Phase Transformations in Carbon Steel. Materials Transactions, 2015, 56, 1461-1466.	1.2	18
42	Atomistic Analyses of Competition between Site-Selective Segregation and Association of Point Defects at Grain Boundary in Y <sub>2</sub> O <sub>3</sub> -Doped ZrO <sub>2</sub> . Materials Transactions, 2015, 56, 1344-1349.	1.2	7
43	Concurrent γ-Phase Nucleation as a Possible Mechanism of δ-γ Massive-like Phase Transformation in Carbon Steel: Numerical Analysis Based on Effective Interface Energy. Materials Transactions, 2015, 56, 1467-1474.	1.2	17
44	Yet Another Marked Difference among Impurities as Modifier Elements for Refinement of Eutectic Si in Al-Si Alloys. Materials Transactions, 2015, 56, 1475-1483.	1.2	5
45	Optical properties and core state of AlNâ€BN ternary compound by <i>ab initio</i> calculations. Physica Status Solidi C: Current Topics in Solid State Physics, 2015, 12, 647-650.	0.8	1
46	Application of a macroscopic model to predict the band segregation induced by shear deformation of semisolid. IOP Conference Series: Materials Science and Engineering, 2015, 84, 012011.	0.6	0
47	Influence of Mg on Solidification of Hypereutectic Cast Iron: X-ray Radiography Study. Metallurgical and Materials Transactions A: Physical Metallurgy and Materials Science, 2015, 46, 4937-4946.	2.2	28
48	Localization of shear strain and shear band formation induced by deformation in semi-solid Al-Cu alloys. IOP Conference Series: Materials Science and Engineering, 2015, 84, 012078.	0.6	1
49	On modeling of grain boundary segregation in aliovalent cation doped ZrO2: Critical factors in site-selective point defect occupancy. Scripta Materialia, 2015, 102, 91-94.	5.2	9
50	Kinetics of the δJγ interface in the massive-like transformation in Fe-0.3C-0.6Mn-0.3Si alloys. IOP Conference Series: Materials Science and Engineering, 2015, 84, 012062.	0.6	19
51	Impact of interplay between magnetic field, transformation strain, and coarsening on variant selection inL10-type FePd. Journal of Applied Physics, 2014, 115, 073501.	2.5	6
52	In Situ Observation of Deformation in Semi-solid Fe-C Alloys at High Shear Rate. Metallurgical and Materials Transactions A: Physical Metallurgy and Materials Science, 2014, 45, 5613-5623.	2.2	17
53	Impact of Dynamic Interlayer Interactions on Thermal Conductivity of Ca3Co4O9. Journal of Electronic Materials, 2014, 43, 1905-1915.	2.2	8
54	Nonrandom Point Defect Configurations and Driving Force Transitions for Grain Boundary Segregation in Trivalent Cation Doped ZrO <sub>2</sub> . Langmuir, 2014, 30, 14179-14188.	3.5	20

#	Article	IF	CITATIONS
55	In Situ Observation of Solidification Behaviors in Carbon Steels Using Synchrotron X-ray Imaging. Materia Japan, 2014, 53, 467-470.	0.1	Ο
56	Characterization of Shear Deformation Based on In-situ Observation of Deformation in Semi-solid Al–Cu Alloys and Water-particle Mixture. ISIJ International, 2013, 53, 1195-1201.	1.4	21
57	Effect of Spatial Distribution of Local Magnetization on Microstructure Formation in <i>L</i> 1 <sub>0</sub> -type Ferromagnetic Alloys under External Magnetic Field. Transactions of the Materials Research Society of Japan, 2013, 38, 673-676.	0.2	3
58	Characterization of Shear Deformation Based on In-situ Observation of Deformation in Semi-Solid Al-Cu Alloys and Water-Particle Mixture. Tetsu-To-Hagane/Journal of the Iron and Steel Institute of Japan, 2013, 99, 141-148.	0.4	2
59	In-situobservation of peritectic solidification in Sn-Cd and Fe-C alloys. IOP Conference Series: Materials Science and Engineering, 2012, 27, 012084.	0.6	25
60	Macroscopic modelling of semisolid deformation for considering segregation bands induced by shear deformation. IOP Conference Series: Materials Science and Engineering, 2012, 33, 012053.	0.6	5
61	Direct Observation of Shear Deformation in Semi-solid Alloys Using X-ray Imaging. Materia Japan, 2012, 51, 561-568.	0.1	1
62	Phase-Field Study of Ordered Domain Growth and Segregation in Intermetallics. Materia Japan, 2012, 51, 53-61.	0.1	0
63	Massive transformation from <i>δ</i> phase to <i>γ</i> phase in Fe–C alloys and strain induced in solidifying shell. IOP Conference Series: Materials Science and Engineering, 2012, 33, 012036.	0.6	38
64	Atomic-level modeling and computation of intergranular glassy film in high-purity Si3N4 ceramics. Journal of the European Ceramic Society, 2012, 32, 1301-1311.	5.7	6
65	Development of X-ray Imaging for Observing Solidification of Carbon Steels. ISIJ International, 2011, 51, 402-408.	1.4	100
66	放射光ã,'å^©ç"¨ã⊷ãŸã,¢ãƒ«ãƒŸãƒ«ã,¦ãƒå•́金ã®å‡å»°ç¾è±¡ã®è§£æ~Ž. Keikinzoku/Journal of Japan Institu	ute@ALigh	t Mætals, 201
67	Direct observation of deformation in semi-solid carbon steel. Scripta Materialia, 2011, 64, 1129-1132.	5.2	81
68	Impurity and vacancy segregation at symmetric tilt grain boundaries in Y2O3-doped ZrO2. Journal of Materials Science, 2011, 46, 4176-4190.	3.7	40
69	In situ investigation of unidirectional solidification in Sn–0.7Cu and Sn–0.7Cu–0.06Ni. Acta Materialia, 2011, 59, 4043-4054.	7.9	56
70	Phase-Field Simulation of Antiphase Boundary Migration in Intermetallic Compounds with Solute and Vacancy Segregation. Materials Research Society Symposia Proceedings, 2011, 1295, 437.	0.1	3
71	Effect of impurity atoms on α2/γ lamellar interfacial misfit in Ti–Al alloy: a systematic first principles study. Philosophical Magazine, 2011, 91, 3685-3704.	1.6	7
72	Local Atomic Configuration of Dislocation-Accumulated Grain Boundary and Energetics of Gradual Transition from Low Angle to High Angle Grain Boundary in Pure Aluminum by First-Principles Calculations. Materials Transactions, 2010, 51, 51-57.	1.2	7

MASATO YOSHIYA

#	Article	IF	CITATIONS
73	Numerical Analyses of Effectiveness of Magnetic Field on Variant Selection in FePd by Phase Field Modeling. ISIJ International, 2010, 50, 1908-1913.	1.4	5
74	Selective dissolution of nanolamellar Ti–41 at.% Al alloy single crystals. Acta Materialia, 2010, 58, 2876-2886.	7.9	25
75	A First-Principles Study of the Role of Na Vacancies in the Thermoelectricity of Na x CoO2. Journal of Electronic Materials, 2010, 39, 1681-1686.	2.2	12
76	Effect of Ionic Radius and Resultant Two-Dimensionality of Phonons on Thermal Conductivity in M x CoO2 (MÂ=ÂLi, Na, K) by Perturbed Molecular Dynamics. Journal of Electronic Materials, 2010, 39, 1439-1445.	2.2	11
77	Derivation of Interatomic Potentials from <i>Ab-initio</i> Calculations for Molecular Dynamics Simulations of Na <sub>X</sub> CoO <sub>2</sub> . Transactions of the Materials Research Society of Japan, 2010, 35, 205-208.	0.2	7
78	Regular Structure Formation of Hypermonotectic Al-In Alloys. Materials Science Forum, 2010, 649, 131-136.	0.3	4
79	Theoretical study on the structure and energetics of intergranular glassy film in Si <sub>3</sub> N <sub>4</sub> -SiO <sub>2</sub> ceramics. International Journal of Materials Research, 2010, 101, 57-65.	0.3	9
80	The role of trace element segregation in the eutectic modification of hypoeutectic Al–Si alloys. Journal of Alloys and Compounds, 2010, 489, 415-420.	5.5	132
81	Trapping of oxygen vacancy at grain boundary and its correlation with local atomic configuration and resultant excess energy in barium titanate: A systematic computational analysis. Physical Review B, 2010, 82, .	3.2	52
82	In-situ Observation of Sn alloy solidification at SPring-8. Yosetsu Gakkai Shi/Journal of the Japan Welding Society, 2009, 78, 600-603.	0.1	2
83	Three-dimensional alignment of FeSi <sub>2</sub> with orthorhombic symmetry by an anisotropic magnetic field. Journal of Physics: Conference Series, 2009, 165, 012021.	0.4	13
84	<i>In situ</i> observation of solidification phenomena in Al–Cu and Fe–Si–Al alloys. International Journal of Cast Metals Research, 2009, 22, 15-21.	1.0	81
85	Formation and microstructure of Al <sub>2</sub> O <sub>3</sub> -YAG eutectic ceramics by phase transformation from metastable system to equilibrium system. Journal of Physics: Conference Series, 2009, 165, 012006.	0.4	5
86	Crystal growth in the bulk-metallic-glass Zr-based alloys by using the DC + AC levitation method. Journal of Physics: Conference Series, 2009, 144, 012056.	0.4	1
87	Design of Mold Materials with Excellent Releasability for IC Encapsulation using Epoxy Compounds. , 2008, , .		0
88	<i>In situ</i> observation of nucleation, fragmentation and microstructure evolution in Sn–Bi and Al–Cu alloys. International Journal of Cast Metals Research, 2008, 21, 125-128.	1.0	48
89	xmlns:mml="http://www.w3.org/1998/Math/MathML" display="inline"> <mml:mrow><mml:msub><mml:mi mathvariant="normal"&gt;Mg<mml:mrow><mml:mn>1</mml:mn><mml:mo>â^'</mml:mo><mml:mi> mathvariant="normal"&gt;Zn</mml:mi><mml:mi>x</mml:mi>solid solutions. Physical Review B. 2007.</mml:mrow></mml:mi </mml:msub></mml:mrow>		
90	76 Effect of the Melt Flow on the Solidified Structure of Middle Carbon Steel by Means of the Levitation Method Using Alternating and Static Magnetic Fields. ISIJ International, 2007, 47, 612-618.	1.4	14

#	Article	IF	CITATIONS
91	Boron addition effects on aluminum nitride fabricated by radio-frequency plasma-assisted molecular beam epitaxy. Physica Status Solidi C: Current Topics in Solid State Physics, 2007, 4, 2486-2489.	0.8	5
92	Oxide ion diffusion in perovskite-structured Ba1â^'xSrxCo1â^'yFeyO2.5: A molecular dynamics study. Solid State Ionics, 2007, 177, 3425-3431.	2.7	39
93	Three-dimensional Observation of Al <sub>2</sub> O <sub>3</sub> -GAP Eutectic Structure by X-ray Micro CT. Materia Japan, 2007, 46, 819-819.	0.1	1
94	Texture and microstructure of ZrO2-4mol% Y2O3 layers obliquely deposited by EB-PVD. Surface and Coatings Technology, 2006, 200, 2725-2730.	4.8	24
95	Thermal Conductivity of Zirconia for Thermal Barrier Coatings: A Perturbed Molecular Dynamics Study. Key Engineering Materials, 2006, 317-318, 521-524.	0.4	5
96	Influence of Number of Layers on Thermal Properties of Nano-Structured Zirconia Film Fabricated by EB-PVD Method. Nippon Kinzoku Gakkaishi/Journal of the Japan Institute of Metals, 2005, 69, 56-60.	0.4	1
97	Anisotropy of Thermal Conductivity in Pure and Y2O3-doped ZrO2 by Perturbed Molecular Dynamics. Nippon Kinzoku Gakkaishi/Journal of the Japan Institute of Metals, 2005, 69, 61-66.	0.4	1
98	A new model of imprint mechanism in ferroelectric memory. Materials Research Society Symposia Proceedings, 2005, 902, 1.	0.1	0
99	Numerical analysis of solute segregation atΣ5(310)â^•[001]symmetric tilt grain boundaries inY2O3-dopedZrO2. Physical Review B, 2005, 71, .	3.2	36
100	Direct observation of intergranular cracks in sintered silicon nitride. Philosophical Magazine, 2004, 84, 2767-2775.	1.6	24
101	Perturbed Molecular Dynamics for Calculating Thermal Conductivity of Zirconia. Molecular Simulation, 2004, 30, 953-961.	2.0	27
102	Evaluation of thermal conductivity of zirconia coating layers deposited by EB-PVD. Journal of Materials Science, 2004, 39, 1823-1825.	3.7	19
103	Phase stability of BaCo1?yFeyO3?? by first principles calculations. Solid State Ionics, 2004, 172, 159-163.	2.7	20
104	Computer simulation of nano-pore formation in EB-PVD thermal barrier coatings. Surface and Coatings Technology, 2004, 187, 399-407.	4.8	16
105	Theoretical prediction of ELNES/XANES and chemical bondings of AlN polytypes. Micron, 2003, 34, 249-254.	2.2	41
106	Atomic structures and bondings of β- and spinel-Si6â^'zAlzOzN8â^'zby first-principles calculations. Physical Review B, 2002, 66, .	3.2	30
107	First principles calculation of ELNES by LCAO methods. Journal of Electron Microscopy, 2002, 51, S107-S112.	0.9	8
108	Fracture and Fatigue Behavior at Ambient and Elevated Temperatures of Alumina Bonded with Copper/Niobium/Copper Interlayers. Journal of the American Ceramic Society, 2002, 85, 2531-2541.	3.8	17

MASATO YOSHIYA

#	Article	IF	CITATIONS
109	Theoretical Prediction of the Structure and Properties of Cubic Spinel Nitrides. Journal of the American Ceramic Society, 2002, 85, 75-80.	3.8	90
110	Theoretical Study on the Chemistry of Intergranular Glassy Film in Si <sub>3</sub> N <sub>4</sub> –SiO <sub>2</sub> Ceramics. Journal of the American Ceramic Society, 2002, 85, 109-112.	3.8	39
111	Electron-energy-loss near edge structures of six-fold-coordinated Zn in MgO. Ultramicroscopy, 2001, 86, 363-370.	1.9	38
112	Prediction of spinel structure and properties of single and double nitrides. Physical Review B, 2001, 63, .	3.2	92
113	Energetical role of modeled intergranular glassy film in Si3N4–SiO2 ceramics. Acta Materialia, 2000, 48, 4641-4645.	7.9	22
114	Core-hole effects on theoretical electron-energy-loss near-edge structure and near-edge x-ray absorption fine structure of MgO. Physical Review B, 2000, 61, 2180-2187.	3.2	98
115	Prediction of the new spinel phase ofTi3N4andSiTi2N4and the metal-insulator transition. Physical Review B, 2000, 61, 10609-10614.	3.2	50
116	Theoretical Calculation of B-K ELNES(Electron Energy Loss Near Edge Structure) from 3d Transition Metal-Boron Systems. Nippon Kinzoku Gakkaishi/Journal of the Japan Institute of Metals, 2000, 64, 527-534.	0.4	0
117	Theoretical calculation of oxygen K electron-energy-loss near-edge structures of Si-doped MgO. Journal of Physics Condensed Matter, 1999, 11, 5661-5670.	1.8	6
118	First principles calculation of chemical shifts in ELNES/NEXAFS of titanium oxides. Journal of Physics Condensed Matter, 1999, 11, 3217-3228.	1.8	62
119	Atomic Structure and Chemical Bondings of Intergranular Glassy Film in Si <sub>3</sub> N <sub>4</sub> -SiO <sub>2</sub> Ceramics. Key Engineering Materials, 1999, 175-176, 107-118.	0.4	1
120	First-principles calculations of electron-energy-loss near-edge structure and near-edge x-ray-absorption fine structure of BN polytypes using model clusters. Physical Review B, 1999, 60, 4944-4951.	3.2	61
121	Chemical bonding of oxygen in intergranular amorphous layers in high-purity β-SiC ceramics. Acta Materialia, 1999, 47, 1281-1287.	7.9	21
122	Structural Study of Thin Amorphous SiO2 and Si3N4 Films by the Grazing Incidence X-Ray Scattering (GIXS) Method. High Temperature Materials and Processes, 1999, 18, 99-107.	1.4	5
123	Interpretation of Siâ€L2,3 Edge Electron Energy Loss Near Edge Structures (ELNES) from Intergranular Glassy Film of Si3N4 Ceramics. Journal of the American Ceramic Society, 1999, 82, 3231-3236.	3.8	23
124	Six-fold coordinated silicon at grain boundaries in sintered α-Al2O3. Applied Physics Letters, 1998, 72, 191-193.	3.3	8
125	Cluster calculation of oxygenK-edge electron-energy-loss near-edge structure of NiO. Physical Review B, 1998, 58, 9693-9696.	3.2	26
126	Improving Releasability of Mold Materials for IC Encapsulation Using Epoxy Compounds. Materials Science Forum, 0, 706-709, 2529-2534.	0.3	0